

# From Image to Video Approximation by Adaptive Splines over Tetrahedralizations

Armin Iske

Department of Mathematics, University of Hamburg  
Bundesstraße 55, 20146 Hamburg, Germany  
armin.iske@uni-hamburg.de

Niklas Wagner

Department of Mathematics, University of Hamburg  
Bundesstraße 55, 20146 Hamburg, Germany  
niklas.wagner@uni-hamburg.de

## Abstract

In previous work [3], we proved asymptotically optimal  $N$ -term approximation rates for image approximation by linear splines over anisotropic triangulations. In this paper, we generalize our previous results from image approximation to video approximation, i.e., from the approximation of bivariate to trivariate target functions. We show that the  $N$ -term approximation rates can be maintained, although we cannot prove their optimality.

*Key words and phrases* : video approximation,  $\alpha$ -horizon function, linear splines, Delaunay triangulations and tetrahedralizations

*2010 AMS Mathematics Subject Classification.* 41A25, 42C40, 94A12

## 1 Introduction

Sparse signal approximation requires suitable dictionaries  $\mathcal{A} = \{\varphi_j\}_{j \in \mathbb{N}}$  to obtain efficient representations of signals  $f$  by  $N$ -term approximations of the form

$$f_N = \sum_{j \in I_N} \alpha_j \varphi_j, \quad (1)$$

where  $N = |I_N| \in \mathbb{N}$  is the size of the index set  $I_N \subset \mathbb{N}$ . The quality of an  $N$ -term approximation (1) is often measured by *rate-distortion curves*, reflecting the required amount of data (measured e.g. in file size of stored information) versus the approximation quality (measured e.g. in *peak signal-to-noise ratio* (PSNR) or in *structural similarity index* (SSIM)).

From a viewpoint of approximation theory, one important quality indicator is the decay rate of asymptotic  $N$ -term approximations  $\{f_N\}_{N \in \mathbb{N}}$  in (1) that are obtained from the chosen dictionary  $\mathcal{A}$ . Popular methods for  $N$ -term image approximations can be found in [1, 5, 6, 11, 12].

In previous work [3, 10], we proposed  $N$ -term image approximations with optimal decay rates for relevant classes of target functions  $f$ , including bivariate horizon functions across  $\alpha$ -Hölder smooth horizon boundaries. The decay rates in [3] were obtained from error estimates of the form

$$\|f - f_N\|_{L^2([0,1]^2)}^2 = \mathcal{O}(N^{-\alpha}) \quad \text{for } N \rightarrow \infty, \quad (2)$$

where  $f_N$  is a (bivariate) linear spline over an anisotropic Delaunay triangulation. In this case, the dictionary  $\mathcal{A}$  is generated by all possible linear spline spaces over conformal triangulations that are covering the image domain. Therefore, the dictionary  $\mathcal{A}$  is very large.

But in [2, 4] we proposed an efficient image approximation algorithm of complexity  $\mathcal{O}(N \log(N))$ , termed *adaptive thinning* (AT), to compute a suitable sequence of spline spaces  $\{\mathcal{S}_N\}_{N \in \mathbb{N}}$  over anisotropic Delaunay triangulations which are locally adapted to the geometry of the image. Our constructive approach in [2, 4] outputs a sequence of image approximations  $f_N \in \mathcal{S}_N$  that are well-adapted to the local regularity of the target function  $f$ .

In this paper, we generalize the approximation method of [3, 10] from image to video approximation, i.e., from the approximation of *bivariate* functions to the approximation of *trivariate* functions. To this end, we first introduce a class of piecewise affine-linear trivariate horizon functions, with singularities along  $\alpha$ -Hölder smooth surfaces. We approximate these prototypical test functions by linear splines over anisotropic tetrahedralizations. Moreover, we show how to maintain the decay rates of the asymptotic  $N$ -term approximations in (2).

## 2 Linear Splines over Conformal Tetrahedralizations

We begin our discussion with the introduction of conformal tetrahedralizations.

**Definition 1.** For a finite point set  $Y \subset \mathbb{R}^3$ , a conformal tetrahedralization is a finite set  $\mathcal{T} \equiv \mathcal{T}_Y = \{T\}_{T \in \mathcal{T}}$  of tetrahedra satisfying the following properties.

- (a) the vertex set of  $\mathcal{T}$  is  $Y$ ;
- (b) two distinct tetrahedra in  $\mathcal{T}$  intersect at most at one common vertex, at one common edge or at one common triangle;
- (c) the convex hull  $\text{conv}(Y)$  of  $Y$  coincides with the area covered by the union of the tetrahedra in  $\mathcal{T}$ .

The conformal Delaunay tetrahedralizations are very important special cases.

**Definition 2.** For a finite point set  $Y \subset \mathbb{R}^3$ , a conformal tetrahedralization  $\mathcal{D}$  of  $Y$  is referred to as Delaunay tetrahedralization of  $Y$ , iff no circumsphere of a tetrahedron  $T \in \mathcal{D}$  contains any point from  $Y$  in its interior.

We recall only a few important facts about Delaunay tetrahedralizations.

- (a) The Delaunay tetrahedralization  $\mathcal{D}$  of  $Y$  is unique, if the point set  $Y$  satisfies the *Delaunay criterion*, i.e., no five points in  $Y$  are co-spherical.
- (b) Delaunay tetrahedralizations can be computed by efficient algorithms.

We remark that for video data, the points in  $Y$  do not satisfy the Delaunay criterion in (a), i.e., there are five co-spherical points in  $Y$ . Due to a generic procedure termed *simulation of simplicity* [8], however, uniqueness can always be enforced even for degenerate sets of data  $Y$ . Therefore, we assume from now and without loss of generality that the Delaunay tetrahedralization  $\mathcal{D}$  is unique. As regards property (b), the Delaunay tetrahedralization  $\mathcal{D}$  for a given point set  $Y$  of size  $N = |Y|$  can be computed in  $\mathcal{O}(N)$  steps on average [7], although the worst case complexity is  $\mathcal{O}(N^2)$  [9, 13].

To explain another important property of Delaunay tetrahedralizations, we first introduce Voronoi diagrams (see [13] for more details).

**Definition 3.** For a finite point set  $Y \subset \mathbb{R}^3$ , the Voronoi diagram  $\mathcal{V} \equiv \mathcal{V}_Y$  of  $Y$  is a cell complex consisting of the Voronoi polytopes

$$V_{\mathbf{y}} \equiv V_{\mathbf{y}}(Y) = \left\{ \mathbf{x} \in \mathbb{R}^3 : \|\mathbf{x} - \mathbf{y}\|_2 = \min_{\mathbf{z} \in Y} \|\mathbf{x} - \mathbf{z}\|_2 \right\} \quad \text{for } \mathbf{y} \in Y,$$

i.e.,  $V_{\mathbf{y}}$  contains all points in  $\mathbb{R}^3$  whose closest point from  $Y$  is  $\mathbf{y}$ .

Another property of the Delaunay tetrahedralization  $\mathcal{D}$  of  $Y$  is as follows.

- (c) The *Voronoi diagram*  $\mathcal{V}$  of  $Y$  is dual to the Delaunay tetrahedralization  $\mathcal{D}$ .

To explain property (c), two distinct points  $\mathbf{y}_i, \mathbf{y}_j \in Y$  are said to be *Voronoi neighbours*, iff the intersection  $V_{\mathbf{y}_i} \cap V_{\mathbf{y}_j}$  is a non-degenerate surface in  $\mathcal{V}$ . Then, the straight line  $[\mathbf{y}_i, \mathbf{y}_j]$  between  $\mathbf{y}_i$  and  $\mathbf{y}_j$  is a Delaunay edge, i.e., the connection between all Voronoi neighbours yields the Delaunay tetrahedralization  $\mathcal{D}$  of  $Y$ . Note that  $[\mathbf{y}_i, \mathbf{y}_j]$  is a Delaunay edge in  $\mathcal{D}$ , iff there is one  $\mathbf{x} \in \mathbb{R}^3$  satisfying

$$\|\mathbf{x} - \mathbf{y}_i\| = \|\mathbf{x} - \mathbf{y}_j\| < \|\mathbf{x} - \mathbf{y}\| \quad \text{for all } \mathbf{y} \in Y \setminus \{\mathbf{y}_i, \mathbf{y}_j\}.$$

In the following, we assume that  $Y \subset \mathbb{R}^3$  is a set of video pixel positions, such that the convex hull  $\text{conv}(Y)$  of  $Y$  coincides with the video domain, which we assume (for simplicity) to be the unit cube  $[0, 1]^3$ , i.e.,  $\text{conv}(Y) = [0, 1]^3$ .

Moreover, we associate with any conformal tetrahedralization  $\mathcal{T}$  of  $Y$  the finite dimensional linear function space of *linear splines* over  $\mathcal{T}$ ,

$$\mathcal{S}_{\mathcal{T}} = \{g \in \mathcal{C}([0, 1]^3) : g|_T \in \mathcal{P}_1 \text{ for all } T \in \mathcal{T}\},$$

consisting of all continuous functions on  $[0, 1]^3$ , whose restriction to any tetrahedron  $T \in \mathcal{T}$  is a linear polynomial in  $\mathcal{P}_1 := \{p : \mathbb{R}^3 \rightarrow \mathbb{R} : p \text{ is affine-linear}\}$ .

Note that for any  $f \in \mathcal{C}([0, 1]^3)$ , there is a unique linear spline interpolant  $s \in \mathcal{S}_{\mathcal{T}}$  to  $f$  over the vertices  $Y$  of  $\mathcal{T}$  satisfying  $s|_Y = f|_Y$ . In particular, any linear spline  $s \in \mathcal{S}_{\mathcal{T}}$  is uniquely determined by its values at the vertices  $Y$  of  $\mathcal{T}$ .

### 3 $N$ -Term Approximation of Horizon Functions

In this section, we discuss  $N$ -term approximation (1) by linear splines  $f_N \in \mathcal{S}_{\mathcal{T}_N}$  over tetrahedralizations  $\mathcal{T}_N$ , for  $N \in \mathbb{N}$ . To this end, we explain how to construct conformal tetrahedralizations  $\{\mathcal{T}_N\}_{N \in \mathbb{N}}$  for vertex sets  $Y_N$ , such that there are constants  $C, M > 0$  (independent of  $N$ ) satisfying the following two properties.

- (a) The size  $|Y_N|$  of  $Y_N$  is bounded by  $|Y_N| \leq M \times N$ ;
- (b) the  $L^2$ -approximation error can be bounded above by

$$\|f - f_N\|_{L^2([0, 1]^3)}^2 \leq CN^{-\alpha},$$

where  $f_N \in \mathcal{S}_{\mathcal{T}_N}$  is the unique linear spline interpolant to  $f$  at  $Y_N$ , and where  $\alpha > 0$  reflects the regularity of  $f$ .

Horizon functions [6] are popular prototypes for piecewise smooth images with discontinuities along Hölder smooth curves, exemplifying edges. To extend the model problem of horizon functions [6] from bivariate functions (i.e., images) to trivariate functions (i.e., videos), we first remark that a bivariate function  $g : [0, 1]^2 \rightarrow \mathbb{R}$  is called *Hölder continuous of order*  $\beta \in (0, 1]$ ,  $g \in \mathcal{C}^\beta([0, 1]^2)$ , iff

$$|g(\mathbf{x}) - g(\mathbf{y})| \leq C\|\mathbf{x} - \mathbf{y}\|^\beta \quad \text{for all } \mathbf{x}, \mathbf{y} \in [0, 1]^2$$

for some  $C > 0$ . Moreover, for  $\alpha = r + \beta$ , with  $r \in \mathbb{N}_0$  and  $\beta \in (0, 1]$ , a function  $g \in \mathcal{C}^r([0, 1]^2)$  is said to be  $\alpha$ -Hölder smooth, iff  $\partial^\gamma g \in \mathcal{C}^\beta([0, 1]^2)$  for all  $\gamma \in \mathbb{N}_0^2$  with  $|\gamma| = r$ . For  $g \in \mathcal{C}^\alpha([0, 1]^2)$ , the semi-norm  $|g|_\alpha$  of  $g$  is given as

$$|g|_\alpha = \inf \left\{ C : |\partial^\gamma g(\mathbf{x}) - \partial^\gamma g(\mathbf{y})| \leq C\|\mathbf{x} - \mathbf{y}\|^\beta \text{ for all } \mathbf{x}, \mathbf{y} \in [0, 1]^2 \right\}.$$

Here we only require  $\alpha \in (1, 2]$ , i.e.,  $\alpha = 1 + \beta$  for  $\beta = \alpha - 1 \in (0, 1]$ . In this case, we have  $\partial^\gamma g \in \mathcal{C}^{\alpha-1}([0, 1]^2)$  for all  $\gamma \in \mathbb{N}_0^2$  with  $|\gamma| = 1$ , where we let

$$|\partial^\gamma g|_{\alpha-1} = |g|_\alpha \quad \text{for } g \in \mathcal{C}^\alpha([0, 1]^2) \text{ and } |\gamma| = 1.$$

Now the class of  $\alpha$ -horizon functions contains all piecewise affine-linear trivariate functions across  $\alpha$ -Hölder smooth horizon surfaces, defined as follows.

**Definition 4.** For any  $\alpha \in (1, 2]$ , a function  $f : [0, 1]^3 \rightarrow \mathbb{R}$  is said to be an  $\alpha$ -horizon function, iff it has the form

$$f(x, y, z) = \begin{cases} p(x, y, z) & \text{for } z \leq g(x, y), \\ q(x, y, z) & \text{otherwise,} \end{cases}$$

for affine-linear  $p, q : \mathbb{R}^3 \rightarrow \mathbb{R}$  and  $g \in \mathcal{C}^\alpha([0, 1]^2)$  satisfying  $g([0, 1]^2) \subset (0, 1)$ . The  $\alpha$ -Hölder smooth surface  $g \in \mathcal{C}^\alpha([0, 1]^2)$  is called horizon boundary of  $f$ .  $\square$

Next we explain the approximation of horizon functions by linear splines over conformal tetrahedralizations. We remark that our approximation scheme can also be applied to piecewise smooth functions with one-dimensional singularities or with point singularities. But for the sake of brevity, we decided to omit this.

### 3.1 Approximation over Conformal Tetrahedralizations

The goal of this section is to construct a sequence  $\{\mathcal{T}_N\}_{N \in \mathbb{N}}$  of tetrahedralizations  $\mathcal{T}_N$  in such a way, that the horizon boundary  $g$  is surrounded by an  $\varepsilon_N$ -corridor  $K_{\varepsilon_N} \subset [0, 1]^3$ . To this end, we interpolate the horizon boundary  $g$  by a second order open B-spline surface  $P_N : [0, 1]^2 \rightarrow \mathbb{R}$ ,

$$P_N(\mathbf{x}) = \sum_{i=0}^n \sum_{j=0}^n D_{i,j} N_{i,1}(x) N_{j,1}(y) \quad \text{for } \mathbf{x} = (x, y), \quad (3)$$

where the samples  $D_{i,j} = (\mathbf{x}_{i,j}, g(\mathbf{x}_{i,j}))$ ,  $0 \leq i, j \leq n$ , are taken over a regular grid in  $[0, 1]^2$  containing  $n^2 = N$  cells. The linear B-splines  $N_{i,1}$ ,  $N_{j,1}$  and their knot vectors are chosen such that  $(\mathbf{x}_{i,j}, P_N(\mathbf{x}_{i,j})) = D_{i,j}$  for  $0 \leq i, j \leq n$ , cf. [15]. We use basic spline approximation to estimate the distance between  $g$  and  $P_N$ .

**Lemma 1.** The  $L^\infty$ -error between  $g$  and its interpolating surface  $P_N$  is bounded above by

$$\|g - P_N\|_{L^\infty([0,1]^2)}^2 \leq CN^{-\alpha/2}.$$

*Proof.* The difference between  $g$  and  $P_N$  can, for  $(x, y) \in [x_i, x_{i+1}] \times [y_j, y_{j+1}]$ , be represented as

$$\begin{aligned} & g(x, y) - P_N(x, y) \\ &= g(x, y) - \sum_{k=i}^{i+1} \sum_{\ell=j}^{j+1} N_{k,1}(x) N_{\ell,1}(y) g(x_k, y_\ell) \\ &= g(x, y) - g(\mathbf{x}_{i,j}) \\ &\quad - n [(x - x_i)(g(\mathbf{x}_{i+1,j}) - g(\mathbf{x}_{i,j})) + (y - y_j)(g(\mathbf{x}_{i,j+1}) - g(\mathbf{x}_{i,j}))] \\ &\quad - n [(x - x_i)(ny - j)(g(\mathbf{x}_{i+1,j}) - g(\mathbf{x}_{i,j}) - g(\mathbf{x}_{i+1,j+1}) + g(\mathbf{x}_{i,j+1}))]. \end{aligned}$$

Since  $g \in \mathcal{C}^\alpha([0, 1]^2)$  we can apply the mean value theorem to obtain

$$\begin{aligned} n [g(\mathbf{x}_{i,j+1}) - g(\mathbf{x}_{i,j})] &= \frac{\partial g}{\partial x_1}(\mathbf{x}_{i,j}) + \mathcal{O}(n^{-(\alpha-1)}) \\ n [g(\mathbf{x}_{i+1,j}) - g(\mathbf{x}_{i,j})] &= \frac{\partial g}{\partial x_2}(\mathbf{x}_{i,j}) + \mathcal{O}(n^{-(\alpha-1)}), \end{aligned}$$

which implies

$$\begin{aligned} g(x, y) - P_N(x, y) &= \\ g(x, y) - g(\mathbf{x}_{i,j}) - (x - x_i) \frac{\partial g}{\partial x_1}(\mathbf{x}_{i,j}) - (y - y_j) \frac{\partial g}{\partial x_2}(\mathbf{x}_{i,j}) &+ \mathcal{O}(n^{-\alpha}). \end{aligned}$$

On the other hand, by Taylor series expansion of  $g(x, y)$  at  $\mathbf{x}_{i,j}$  we have

$$g(x, y) = g(\mathbf{x}_{i,j}) + (x - x_i) \frac{\partial g}{\partial x_1}(\mathbf{x}_{i,j}) + (y - y_j) \frac{\partial g}{\partial x_2}(\mathbf{x}_{i,j}) + \mathcal{O}(n^{-\alpha}),$$

so that (with using the assumption  $n^2 = N$ )

$$|g(x, y) - P_N(x, y)| = \mathcal{O}(n^{-\alpha}) = \mathcal{O}(N^{-\alpha/2}) \quad \text{for all } (x, y) \in [0, 1]^2,$$

which completes our proof.  $\square$

In the following, it will be convenient to let  $\varepsilon_N = N^{-\alpha/2}$ , for  $N \in \mathbb{N}$ . Next we turn to the construction of an  $\varepsilon_N$ -corridor  $K_{\varepsilon_N} \subset [0, 1]^3$  containing the horizon boundary  $g$ . To this end, consider some  $\mathbf{x}' \in [x_i, x_{i+1}] \times [y_j, y_{j+1}]$ . Then, the spline interpolant  $P_N$  of  $g$  in (3) is locally given by a convex combination over the adjacent grid points. In this case, we have the inclusion

$$P_N(\mathbf{x}') \in \text{conv}\{D_{i,j}, D_{i+1,j}, D_{i,j+1}, D_{i+1,j+1}\},$$

where the convex hull  $\text{conv}\{D_{i,j}, D_{i+1,j}, D_{i,j+1}, D_{i+1,j+1}\}$  is a non-degenerate tetrahedron, if the points  $D_{i,j}, D_{i+1,j}, D_{i,j+1}, D_{i+1,j+1}$  are not co-planar.

Due to Lemma 1, the maximum distance between  $P_N$  and  $g$  is (up to a constant independent of  $N$ ) less than  $\varepsilon_N$ . This allows us to construct an  $\varepsilon_N$ -corridor  $K_{\varepsilon_N}$  surrounding the surface  $g$  by offsetting each tetrahedron along the  $z$ -coordinate about offset  $\varepsilon_N$ . In this case, we have

$$g(\mathbf{x}') \in \text{conv}\{D_{k,\ell} \pm (0, 0, \varepsilon_N) : k \in \{i, i+1\}, \ell \in \{j, j+1\}\}.$$

In the following discussion, it will be convenient to let

$$A_{N,i,j} = \text{conv}\{D_{k,\ell} \pm (0, 0, \varepsilon_N) : k \in \{i, i+1\}, \ell \in \{j, j+1\}\}$$

for the convex hull of the  $(i, j)$ -th tetrahedron's offset. By the union of the convex pieces  $A_{N,i,j} \subset [0, 1]^3$  we obtain an  $\varepsilon_N$ -corridor  $A_N = K_{\varepsilon_N}$  satisfying

$$(\mathbf{x}, g(\mathbf{x})) \subset A_N := \bigcup_{0 \leq i, j \leq n-1} A_{N,i,j} \quad \text{for all } \mathbf{x} \in [0, 1]^2.$$

Now the video domain  $[0, 1]^3$  is split into three parts, made up by  $A_N$  and the two subdomains  $A_N^\pm \subset [0, 1]^3$  lying above and below  $A_N$ , respectively. The construction of the point set  $Y_N$  is now a rather straightforward task (as illustrated in Figure 1): For the grid points  $\mathbf{x}_{i,j} \in [0, 1]^2$ ,  $0 \leq i, j \leq n$ , we take for  $Y_N$  the union

$$Y_N = \bigcup_{0 \leq i, j \leq n} \{(\mathbf{x}_{i,j}, 0), D_{i,j} \pm (0, 0, \varepsilon_N), (\mathbf{x}_{i,j}, 1)\}.$$

Therefore, we have  $|Y_N| \leq 4 \times (N + 1)$ . For the construction of the tetrahedralization  $\mathcal{T}_{Y_N}$  of  $Y_N$  we split the grid cells, such that each tetrahedron in  $\mathcal{T}_{Y_N}$  is either contained in  $A_N$ ,  $\mathcal{T}_{Y_N} \subset A_N$ , or outside  $A_N$ , i.e.,  $\mathcal{T}_{Y_N} \subset [0, 1]^3 \setminus A_N$ .

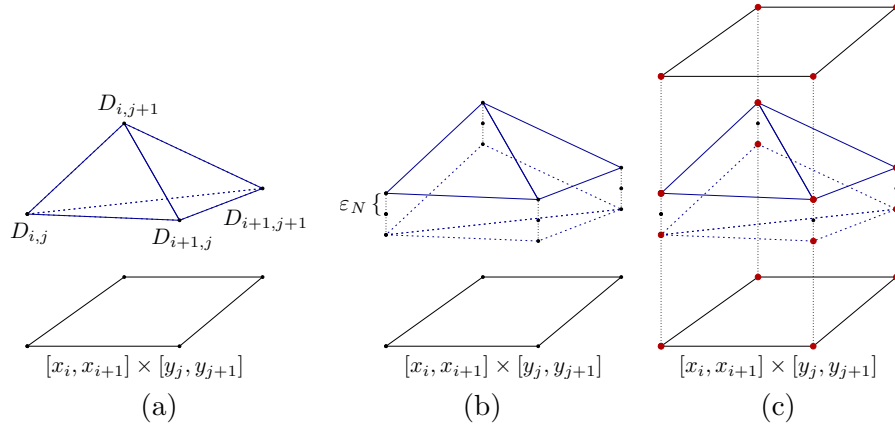


Figure 1: Construction steps for  $Y_N$ : (a)  $\text{conv}\{D_{i,j}, D_{i+1,j}, D_{i,j+1}, D_{i+1,j+1}\}$ ; (b)  $A_{N,i,j}$ , the offset tetrahedron; (c)  $Y_N$  over  $[x_i, x_{i+1}] \times [y_j, y_{j+1}]$ .

Now we are in a position where we can prove the following  $L^2$ -error estimate for conformal tetrahedralizations.

**Proposition 1.** *For  $\alpha \in (1, 2]$ , let  $f : [0, 1]^3 \rightarrow \mathbb{R}$  be an  $\alpha$ -horizon function. Then there exist constants  $C, M > 0$  (independent of  $N$ ), such that for any  $N \in \mathbb{N}$  there exists a tetrahedralization  $\mathcal{T}_N$  with  $|\mathcal{T}_N| \leq M \times N$  vertices satisfying*

$$\|f - f_N\|_{L^2([0,1]^3)}^2 \leq CN^{-\alpha},$$

where  $f_N \in \mathcal{S}_{\mathcal{T}_N}$  interpolates  $f$  at the vertices in  $\mathcal{T}_N$ .

*Proof.* We choose  $\mathcal{T}_N = \mathcal{T}_{Y_N}$  and approximate  $f$  by functions  $f_N$  of the form

$$f_N(\mathbf{x}) = \begin{cases} p(\mathbf{x}) & \text{for } \mathbf{x} \in A_N^- \\ q(\mathbf{x}) & \text{for } \mathbf{x} \in A_N^+ \\ g_N(\mathbf{x}) & \text{for } \mathbf{x} \in A_N \end{cases} \quad \text{for } \mathbf{x} \in [0, 1]^3,$$

where  $g_N$  is the interpolating linear spline to  $f$  at the vertices of the  $\varepsilon_N$ -corridor  $A_N$ . Note that  $f_N$  coincides with  $f$  outside of  $A_N$ , so that

$$\begin{aligned} \|f - f_N\|_{L^2([0,1]^3)}^2 &= \|f - f_N\|_{L^2(A_N)}^2 \\ &= \sum_{0 \leq i,j \leq n-1} \|f - f_N\|_{L^2(A_{N,i,j})}^2 \\ &= \sum_{0 \leq i,j \leq n-1} \sum_{T \in A_{N,i,j}} \|f - f_N\|_{L^2(T)}^2, \end{aligned} \quad (4)$$

where we tetrahedralized the corridor  $A_N$ . Hence, it remains to consider the  $L^2$ -error over each tetrahedron  $T \subset A_N$ .

Now note that the restriction  $f_N|_T$  of  $f_N$  to a tetrahedron  $T$  interpolates  $f$  at the four vertices of  $T$ . Moreover, since both  $f$  and  $f_N$  are affine-linear functions outside the  $\varepsilon_N$ -corridor  $A_N$ , we can bound the  $L^2$ -error on any tetrahedron  $T \in \mathcal{T}_N$  by

$$\|f - f_N\|_{L^2(T)}^2 \leq C \cdot |T| \cdot \|f\|_{L^2(T)}^2,$$

where  $|T|$  is the volume of  $T$  in  $\mathbb{R}^3$ , and where the constant  $C$  is independent of  $N$ . Therefore, the  $L^2$ -error in (4) can be bounded above by

$$\begin{aligned} \|f - f_N\|_{L^2([0,1]^3)}^2 &\leq \sum_{0 \leq i,j \leq n-1} \sum_{T \in A_{N,i,j}} C \cdot |T| \cdot \|f\|_{L^2(T)}^2 \\ &\leq C \sum_{0 \leq i,j \leq n-1} |A_{N,i,j}| \cdot \|f\|_{L^2(A_{N,i,j})}^2. \end{aligned}$$

To bound the volume  $|A_{N,i,j}|$  we recall the construction of  $A_{N,i,j}$ : We offset the convex hull  $D := \text{conv}\{D_{i,j}, D_{i+1,j}, D_{i,j+1}, D_{i+1,j+1}\}$  along the z-coordinate about offset  $\varepsilon_N = CN^{-\alpha/2} = Cn^{-\alpha}$ . Since the grid has mesh width  $n^{-1}$ , we have

$$|A_{N,i,j}| \leq |D| + 2Cn^{-\alpha} \times n^{-1} \times n^{-1}.$$

For  $g \in \mathcal{C}^\alpha([0,1]^2)$  we can, as performed in [14], bound  $|D|$  from above by

$$|D| \leq Cn^{-\alpha} \times n^{-1} \times n^{-1},$$

so that for  $\alpha \in (1, 2]$  we have

$$|A_{N,i,j}| \leq Cn^{-\alpha}n^{-2} \leq CN^{-\alpha}.$$

This finally allows us to refine our estimate on the  $L^2$ -error (4) by

$$\begin{aligned} \|f - f_N\|_{L^2([0,1]^3)}^2 &\leq C \sum_{0 \leq i,j \leq n-1} |A_{i,j,N}| \cdot \|f\|_{L^2(A_{i,j,N})}^2 \\ &\leq C \sum_{0 \leq i,j \leq n-1} N^{-\alpha} \cdot \|f\|_{L^2(A_{i,j,N})}^2 \\ &\leq CN^{-\alpha} \|f\|_{L^2(A_N)}^2 \leq CN^{-\alpha} \|f\|_{L^2([0,1]^3)}^2. \end{aligned}$$

□



### 3.2 Approximation over Delaunay Tetrahedralizations

Now we turn to the construction of Delaunay tetrahedralizations, where we wish to maintain the asymptotic  $L^2$  error estimate of Proposition 1. To this end, recall that in our construction of conformal tetrahedralizations, any tetrahedron  $T \in \mathcal{T}_N$  is either fully contained in  $A_N$  or outside of  $A_N$ , i.e.,

$$T \cap A_N \neq \emptyset \implies T \subset A_N \quad \text{for all } T \in \mathcal{T}_N. \quad (5)$$

For the construction of the (more restrictive) Delaunay tetrahedralizations of  $Y_N$ , we can no longer maintain property (5). Recall the duality between the Delaunay tetrahedralization  $\mathcal{D}$  of  $Y_N$  and its Voronoi diagram, see property (c) in Section 2. According to this duality relation, any edge in  $\mathcal{D}$  connecting points  $\mathbf{y}_i, \mathbf{y}_j \in Y_N$  satisfies the Delaunay property, iff there exists one  $\mathbf{x} \in \mathbb{R}^3$  satisfying

$$\|\mathbf{x} - \mathbf{y}_i\| = \|\mathbf{x} - \mathbf{y}_j\| < \|\mathbf{x} - \mathbf{y}\| \quad \text{for all } \mathbf{y} \in Y \setminus \{\mathbf{y}_i, \mathbf{y}_j\}. \quad (6)$$

Suppose  $T \in \mathcal{D}$  is a tetrahedron which does not satisfy (5), i.e.,  $T \cap A_N \neq \emptyset$  and  $T \cap ([0, 1]^3 \setminus A_N) \neq \emptyset$ . Then, there is at least one edge  $e$  in  $T$  passing through the boundary of  $A_N$ , and so there is one point  $\mathbf{x} \in e$  satisfying (6). In this situation, two scenarios are possible (as illustrated in Figure 2):

- (a)  $|g|_\alpha$  is large, resulting in large local variations of  $\partial_x g$  or  $\partial_y g$ ;
- (b)  $\partial_x g$  and  $\partial_y g$  are independent, where their deviation  $|\partial_x g - \partial_y g|$  is large.

To maintain property (5), we can construct a refinement of  $Y_N$  as follows.

**Lemma 2.** *Let  $f : [0, 1]^3 \rightarrow \mathbb{R}$  be an  $\alpha$ -horizon function for  $\alpha \in (1, 2]$ . Then there is a refinement  $Z_N$  of the point set  $Y_N$ , where  $|Z_N| \leq M \times N$  (with  $M$  independent of  $N$ ), such that any tetrahedron  $T$  in the Delaunay tetrahedralization  $\mathcal{D}_{Z_N}$  of  $Z_N$  satisfies property (5).*

*Proof.* We construct the refinement  $Z_N$  of  $Y_N$  as follows. We subdivide each cell of the regular grid, for some  $a, u, v \in \mathbb{N}$  independent of  $N$  (to be specified later), into  $av$  cells along the x-coordinate and into  $au$  cells along the y-coordinate. The refined point set  $Z_N$  is then given by the union of all vertices on the upper and lower boundary of  $A_N$  and the video domain  $[0, 1]^3$  over the refined grid. As we will show, these vertices are close enough to prevent undesired Delaunay edges violating property (5), see Figure 3.

The resulting refinement  $Z_N$  of  $Y_N$  satisfies the bound

$$|Z_N| \leq av \times au \times |Y_N| \leq av \times au \times 4 \times (N + 1),$$

in which case the size  $|Z_N|$  of  $Z_N$  grows only linearly in  $N$ , as required.

Yet it remains to show that every tetrahedron  $T \in \mathcal{D}(Z_N)$  satisfies property (5).

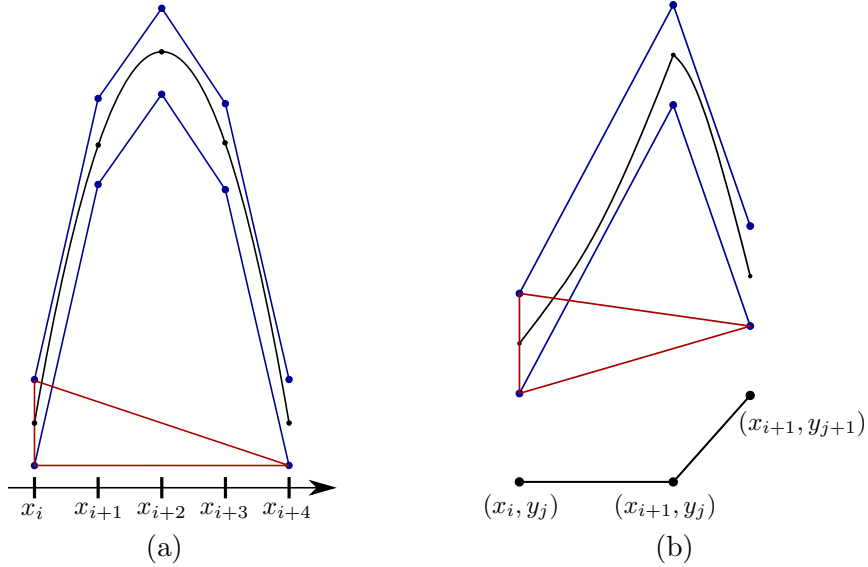


Figure 2: Delaunay edges (red) not satisfying property (5) for following reasons: (a) for large  $|g|_\alpha$ , here visualised for one a lateral surface; (b) for large  $|\partial_x g - \partial_y g|$ .

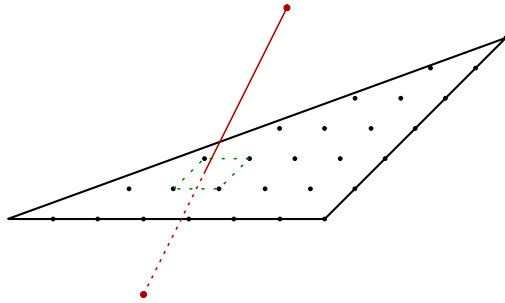


Figure 3: Refinement of  $Y_N$  yields vertices that close enough to split the edge  $e$ .

To prove this, suppose that a tetrahedron  $T \in \mathcal{D}_{Z_N}$  does not satisfy (5). Then there exists a Delaunay edge  $e$  in  $T$  passing through the boundary of  $A_N$ . Let  $\mathbf{z}_1, \mathbf{z}_2 \in Z_N$  be the vertices connected by  $e$ , and let  $\mathbf{x} \in [0, 1]^3$  be a point where  $e$  intersects the boundary of  $A_N$ . Since  $e$  is a Delaunay edge, the points  $\mathbf{z}_1$  and  $\mathbf{z}_2$  are Voronoi neighbours. In this case, any point on  $e$ , in particular  $\mathbf{x}$ , is closer to  $\mathbf{z}_1$  or  $\mathbf{z}_2$  than any other point  $\mathbf{z} \in Z_N$ .

Without loss of generality we assume  $\|\mathbf{z}_1 - \mathbf{x}\|_2 \leq \|\mathbf{z}_2 - \mathbf{x}\|_2$ . Moreover,  $\mathbf{z}_1 \in A_{N,i,j}$  for some  $0 \leq i, j \leq n$ . Now we can represent  $\mathbf{z}_1 \in Z_N$  as

$$\mathbf{z}_1 = \left( x_i + \frac{k}{nav}, y_j + \frac{\ell}{nau}, H_{\mathbf{z}_1} \right)$$

for some  $k, \ell \in \mathbb{N}$  and  $H_{\mathbf{z}_1} \in [0, 1]$ . Moreover, we let

$$s_{i,j,x} = \frac{g(\mathbf{x}_{i+1,j}) - g(\mathbf{x}_{i,j})}{\|\mathbf{x}_{i+1,j} - \mathbf{x}_{i,j}\|_2} = n(g(\mathbf{x}_{i+1,j}) - g(\mathbf{x}_{i,j})),$$

denote the slope of the linear spline between samples  $D_{i,j}$  and  $D_{i+1,j}$ . Likewise,

$$s_{i,j,y} = \frac{g(\mathbf{x}_{i,j+1}) - g(\mathbf{x}_{i,j})}{\|\mathbf{x}_{i,j+1} - \mathbf{x}_{i,j}\|_2} = n(g(\mathbf{x}_{i,j+1}) - g(\mathbf{x}_{i,j})),$$

denotes the slope of the linear spline between  $D_{i,j}$  and  $D_{i,j+1}$ . Due to the mean value theorem we have  $s_{i,j,x} \leq \|\partial_x g\|_{\infty, [0,1]^2}$  and  $s_{i,j,y} \leq \|\partial_y g\|_{\infty, [0,1]^2}$ .

In the remainder of this proof, we determine one  $\mathbf{z}' \in Z_N \setminus \{\mathbf{z}_1, \mathbf{z}_2\}$  satisfying  $\|\mathbf{z}' - \mathbf{x}\|_2 \leq \|\mathbf{z}_1 - \mathbf{x}\|_2$ , in which case  $e$  cannot be an edge in the Delaunay tetrahedralization  $\mathcal{D}_{Z_N}$  of  $Z_N$ .

To this end, we consider the following five cases.

**Case 1:** Suppose  $\mathbf{z}_1 \in A_{N,i,j}^+$  and  $\mathbf{x} \in A_{N,i,j}^+$  or  $\mathbf{x} \in A_{N,i\pm 1,j\pm 1}^+$ .

For  $g \in \mathcal{C}^\alpha([0,1]^2)$  we can rely on arguments similar to those in the proof of Lemma 1: If  $\mathbf{x} \approx \mathbf{y}$  then  $\partial_x g(\mathbf{x}) \approx \partial_x g(\mathbf{y})$  and  $\partial_y g(\mathbf{x}) \approx \partial_y g(\mathbf{y})$ . To be more precise, we can in this case represent the slopes  $s_{k,\ell,x}$  and  $s_{k,\ell,y}$  for any  $k \in \{i-2, \dots, i+2\}$  and  $\ell \in \{j-2, \dots, j+2\}$  as

$$\begin{aligned} s_{k,\ell,x} &= s_{i,j,x} + Cn^{-\beta} = s_{i,j,x} + \mathcal{O}\left(\frac{1}{n^\beta}\right) \\ s_{k,\ell,y} &= s_{i,j,y} + Cn^{-\beta} = s_{i,j,y} + \mathcal{O}\left(\frac{1}{n^\beta}\right). \end{aligned}$$

Note that  $\mathbf{x} \notin Z_N$ , since otherwise  $\mathbf{z}_1$  and  $\mathbf{z}_2$  are not Voronoi neighbours. Therefore, there exist  $b, c \in \mathbb{Z}$ ,  $\Delta_1, \Delta_2 \in [-\frac{1}{2}, \frac{1}{2}]$  and  $H_{\mathbf{x}} \in [0, 1]$  satisfying

$$\mathbf{x} = \left( x_i + \frac{k}{nav} + \frac{b}{nav} + \frac{\Delta_1}{nav}, y_j + \frac{\ell}{nau} + \frac{c}{nau} + \frac{\Delta_2}{nau}, H_{\mathbf{x}} \right).$$

Now let  $\mathbf{z}' \in Z_N$  be a grid point which is closest to  $\mathbf{x}$  by

$$\mathbf{z}' = \left( x_i + \frac{k}{nav} + \frac{b}{nav}, y_j + \frac{\ell}{nau} + \frac{c}{nau}, H_{\mathbf{z}'} \right),$$

for a suitable  $H_{\mathbf{z}'} \in [0, 1]$ , so that  $\mathbf{z}' \in A_{N,i,j}^+$ . In this case we have

$$\left(\frac{1}{na}\right)^2 \|\mathbf{x} - \mathbf{z}'\|_2^2 = \left\| \left( \frac{\Delta_1}{v}, \frac{\Delta_2}{u}, s_{i,j,x} \frac{\Delta_1}{v} + s_{i,j,y} \frac{\Delta_2}{u} + \mathcal{O}(n^{-\beta}) \right) \right\|_2^2 \quad (7)$$

and

$$\begin{aligned} & \left(\frac{1}{na}\right)^2 \|\mathbf{x} - \mathbf{z}_1\|_2^2 \\ &= \left\| \left( \frac{b}{v} + \frac{\Delta_1}{v}, \frac{c}{u} + \frac{\Delta_2}{u}, s_{i,j,x} \left( \frac{b}{v} + \frac{\Delta_1}{v} \right) + s_{i,j,y} \left( \frac{c}{u} + \frac{\Delta_2}{u} \right) + \mathcal{O}(n^{-\beta}) \right) \right\|_2^2 \end{aligned}$$

Now  $\|\mathbf{z}' - \mathbf{x}\|_2 \leq \|\mathbf{z}_1 - \mathbf{x}\|_2$  holds, iff

$$\frac{u}{v}(1 + s_{i,j,x}^2)(b^2 + 2b\Delta_1) + \frac{u}{v}(1 + s_{i,j,y}^2)(c^2 + 2c\Delta_2) + 2s_{i,j,x}s_{i,j,y}(bc + b\Delta_2 + c\Delta_1)$$

is non-negative, for  $n$  large enough. Note that this can be accomplished for suitably chosen  $u/v$ , depending on  $|s_{i,j,x}|$  and  $|s_{i,j,y}|$ , but independent of  $N = n^2$ .

**Case 2:** Suppose  $\mathbf{z}_1 \in A_{N,i,j}^-$ ,  $\mathbf{x} \in A_{N,i,j}^+$ . As in Case 1, we find (7) and

$$\begin{aligned} & \left(\frac{1}{na}\right)^2 \|\mathbf{x} - \mathbf{z}_1\|_2^2 = \\ & \left\| \left( \frac{b}{v} + \frac{\Delta_1}{v}, \frac{c}{u} + \frac{\Delta_2}{u}, s_{i,j,x} \left( \frac{b}{v} + \frac{\Delta_1}{v} \right) + s_{i,j,y} \left( \frac{c}{u} + \frac{\Delta_2}{u} \right) + \mathcal{O}(n^{-\alpha} + n^{-\beta}) \right) \right\|_2^2, \end{aligned}$$

in which case we have  $\|\mathbf{z}' - \mathbf{x}\|_2 \leq \|\mathbf{z}_1 - \mathbf{x}\|_2$  for  $n$  large enough.

**Case 3:** Suppose  $\mathbf{z}_1 \in A_{N,i,j}^-$  and  $\mathbf{x} \in A_{N,i',j'}^+$ , where  $(i, j) \neq (i', j')$ .

We regard the straight line  $e$  between  $\mathbf{z}_1$  and  $\mathbf{x}$ . Since  $[0, 1]^3$  is split into three subdomains  $(A_N, A_N^+$  and  $A_N^-)$ , we have  $e \cap \text{int}(A_N) \neq \emptyset$ .

*Case 3a:* If  $e \cap \text{int}(A_{N,i,j}) \neq \emptyset$ , then there is some  $\mathbf{x}' \in \partial A_{N,i,j} \cap e$ , where  $\mathbf{x} \neq \mathbf{x}'$ . If  $\mathbf{x}' \in A_{N,i,j}^+$  or  $\mathbf{x}' \in A_{N,i,j}^-$ , then we can resort to Case 1 or Case 2, respectively. Otherwise,  $\mathbf{x}'$  lies on a lateral surface of  $A_{N,i,j}$ , whose height is  $CN^{-\alpha}$  (for some  $C$  independent of  $N$ ). In this case, there is (for  $N$  large enough) one  $\mathbf{z}' \in Z_N \cap \partial A_{N,i,j} \setminus \{\mathbf{z}_1, \mathbf{z}_2\}$  satisfying

$$\|\mathbf{z}' - \mathbf{x}'\|_2 \leq \|\mathbf{z}_1 - \mathbf{x}'\|_2.$$

*Case 3b:* If  $e \cap \text{int}(A_{N,i,j}) = \emptyset$ , then  $e \cap A_N^- \neq \emptyset$ , in which case there are  $0 \leq k, \ell \leq n-1$  satisfying  $e \cap A_{N,k,\ell}^- \neq \emptyset$ . In this case we can, for  $\mathbf{x}' \in e \cap A_{N,k,\ell}^-$  and for  $\mathbf{y} = \mathbf{y}'$ , resort to either Case 1 or to Case 2.

**Case 4:** Let  $\mathbf{z}_1 \in A_{N,i,j}^+$ ,  $\mathbf{x} \in A_{N,i',j'}^+$ , where  $A_{N,i,j}^+$  is not adjacent to  $A_{N,i',j'}^+$ . Since  $\mathbf{x}$  and  $\mathbf{z}_1$  are not in adjacent  $A_{N,i,j}$ , we immediately obtain  $\|\mathbf{x} - \mathbf{z}_1\|_2^2 \geq n^{-2}$ .

Choosing  $z'$  as in Case 1, we obtain

$$\begin{aligned}\|\mathbf{x} - \mathbf{z}'\|_2^2 &= \left\| \left( \frac{\Delta_1}{nav}, \frac{\Delta_2}{nau}, s_{i,j,x} \frac{\Delta_1}{nav} + s_{i,j,y} \frac{\Delta_2}{nau} \right) \right\|_2^2 \\ &\leq \left\| \left( \frac{1}{an}, \frac{1}{an}, |g|_\alpha \frac{1}{an} + |g|_\alpha \frac{1}{an} \right) \right\|_2^2 \\ &= \frac{2}{(an)^2} + \frac{4}{(an)^2} |g|_\alpha^2 = \frac{1}{(an)^2} (2 + 4|g|_\alpha^2),\end{aligned}$$

on the one hand. On the other hand we have (for  $a$  large enough)

$$\|\mathbf{x} - \mathbf{z}_1\|_2^2 \geq \frac{1}{n^2} \geq \frac{1}{(an)^2} (2 + 4|g|_\alpha^2).$$

Altogether, we have  $\|\mathbf{z}' - \mathbf{x}\|_2 \leq \|\mathbf{z}_1 - \mathbf{x}\|_2$  for  $a$  large enough.

**Case 5:** In the remaining case, we reflect the  $z$ -coordinate about  $z = 1/2$  to obtain one of the previous cases, Case 1-4.

Now we can complete our proof as follows. Since for each of the above cases, Case 1-5,  $v$  and  $u$  are bounded (where their bounds depend only on  $\|\partial_x g\|_{\infty, [0,1]^2}$  or  $\|\partial_y g\|_{\infty, [0,1]^2}$ ) and since, moreover,  $a$  depends only on  $|g|_\alpha$ , we have established the bound

$$|Z_N| \leq \sum_{0 \leq i, j \leq n-1} (v+1)(u+1)a \leq \sum_{0 \leq i, j \leq n-1} v' u' a \leq v' u' a n^2 = v' u' a N,$$

where  $a, v' := \max\{v\} + 1$  and  $u' := \max\{u\} + 1$  are independent of  $N$ .  $\square$

We can summarize the discussion of this section as follows.

**Theorem 1.** *Let  $f : [0, 1]^3 \rightarrow \mathbb{R}$  be an  $\alpha$ -horizon function, where  $\alpha \in (1, 2]$ . Then there exist constants  $C, M > 0$  independent of  $N$ , such that there is a Delaunay tetrahedralization  $\mathcal{D}_N = \mathcal{D}_{Z_N}$ , with  $|Z_N| \leq M \times N$  for all  $N \in \mathbb{N}$ , satisfying*

$$\|f - f_N\|_{L^2([0,1]^3)}^2 \leq CN^{-\alpha},$$

where  $f_N \in \mathcal{S}_{\mathcal{D}_N}$  is the spline interpolant to  $f$  at  $Z_N$ .  $\square$

We finally remark that our decay rates of Proposition 1 (for conformal tetrahedralizations) and of Theorem 1 (for Delaunay tetrahedralizations) comply with those in [3], as obtained for the bivariate case of image approximation. But we cannot show optimality for our obtained decay rates of video approximation, unlike in [3].

## References

- [1] E. Candés, D. Donoho: New tight frames of curvelets and optimal representations of objects with piecewise  $C^2$  singularities. *Comm. Pure Appl. Math.* **57**(2), 2004, 219–266.
- [2] L. Demaret, N. Dyn, A. Iske: Image compression by linear splines over adaptive triangulations. *Signal Processing* **86**(7), July 2006, 1604–1616.
- [3] L. Demaret, A. Iske: Optimal N-term approximation by linear splines over anisotropic Delaunay triangulations. *Math. Comp.* **84**, 2015, 1241–1264.
- [4] L. Demaret, A. Iske: Adaptive image approximation by linear splines over locally optimal Delaunay triangulations. *IEEE Signal Processing Letters* **13**(5), May 2006, 281–284.
- [5] M.N. Do, M. Vetterli: The contourlet transform: an efficient directional multiresolution image representation. *IEEE Transactions on Image Processing* **14**(12), December 2005, 2091–2106.
- [6] D. Donoho: Wedgelets: nearly-minimax estimation of edges. *Ann. Stat.* **27**, 1999, 859–897.
- [7] R.A. Dwyer: Higher-dimensional Voronoi diagrams in linear expected time. *Discrete Comput. Geom* **6**, 1991, 343–367.
- [8] H. Edelsbrunner, E. Mücke: Simulation of simplicity: a technique to cope with degenerate cases in geometric algorithms. *ACM Transactions on Graphics* **9**(1), 1990, 66–104.
- [9] H. Edelsbrunner, F.P. Preparata, D.B. West: Tetrahedrizing point sets in three dimensions. *Journal of Symbolic Computation* **10**, 1990, 335–347.
- [10] A. Iske, L. Demaret: Optimally sparse image approximation by adaptive linear splines over anisotropic triangulations. *IEEE International Conference on Sampling Theory and Applications (SampTA2015)*, 463–467.
- [11] E. Le Pennec, S. Mallat: Bandelet image approximation and compression. *Multiscale Model. Simul.* **4**, 2005, 992–1039.
- [12] D.D. Po and M.N. Do: Directional multiscale modeling of images using the contourlet transform. *IEEE Trans. Image Proc.* **15**, 2006, 1610–1620.
- [13] F.P. Preparata, M.I. Shamos: *Computational Geometry*. Springer, 1988.
- [14] N. Wagner: *N-Term Approximation by Linear Splines over Anisotropic Delaunay Tetrahedralizations*. M.Sc. Thesis, Univ. of Hamburg, 2016.
- [15] D. Salomon: *Curves and Surfaces for Computer Graphics*. Springer, 2006.